

Article

# Efficient Numerical Methods of Inverse Coefficient Problem Solution for One Inhomogeneous Body

Alexandr Vatulyan , Pavel Uglich, Vladimir Dudarev \*  and Roman Mnuhkin 

Institute of Mathematics, Mechanics and Computer Sciences Named after I.I. Vorovich, Southern Federal University, 8a Milchakova Street, 344090 Rostov-on-Don, Russia; aovatulyan@sfnu.ru (A.V.); puglich@inbox.ru (P.U.); romamnuhin@yandex.ru (R.M.)

\* Correspondence: dudarev\_vv@mail.ru

**Abstract:** In the present paper, the problems of longitudinal and flexural vibrations of an inhomogeneous rod are considered. The Young's modulus and density are variable in longitudinal coordinate. Vibrations are caused by a load applied at the right end. The proposed method allows us to consider a wider class of inhomogeneity laws in comparison with other numerical solutions. Sensitivity analysis is carried out. A new inverse problem related to the simultaneous identification of the variation laws of Young's modulus and density from amplitude–frequency data, which are measured in given frequency ranges, is considered. Its solution is based on an iterative process: at each step, a system of two Fredholm integral equations of the first kind with smooth kernels is solved numerically. The analysis of the kernels is carried out for different frequency values. To find the initial approximation, several approaches are proposed: a genetic algorithm, minimization of the residual functional on a compact set, and additional information about the values of the sought-for functions at the ends of the rod. The Tikhonov regularization and the LSQR method are proposed. Examples of reconstruction of monotonic and non-monotonic functions are presented.

**Keywords:** Tikhonov regularization; LSQR method; inverse problem; Fredholm integral equation; inhomogeneous body

**MSC:** 47A52, 65R30, 74H75, 45B05



**Citation:** Vatulyan, A.; Uglich, P.; Dudarev, V.; Mnuhkin R. Efficient Numerical Methods of Inverse Coefficient Problem Solution for One Inhomogeneous Body. *Axioms* **2023**, *12*, 912. <https://doi.org/10.3390/axioms12100912>

Academic Editor: Babak Shiri and Zahra Alijani

Received: 28 July 2023

Revised: 18 September 2023

Accepted: 20 September 2023

Published: 25 September 2023



**Copyright:** © 2023 by the authors. Licensee MDPI, Basel, Switzerland. This article is an open access article distributed under the terms and conditions of the Creative Commons Attribution (CC BY) license (<https://creativecommons.org/licenses/by/4.0/>).

## 1. Introduction

Nowadays, the study of inverse coefficient problems is an important part of modern mechanics. These problems have wide practical applications in the implementation of nondestructive testing and diagnosis of objects of mass production and critical purposes.

One of the most promising inhomogeneous materials is a functionally graded material (FGM) [1–4]. Their physical properties continuously change along spatial coordinates. This leads to a significantly reduced probability of cracking compared to that of conventional composite laminates. The FGM production is complex, high-tech and includes a few different processes (crushing, pressing, melting, spraying, etc.). In this case, the physical properties of the constituent components change continuously. One way to describe the behavior of such materials is to use a model of linear elasticity theory with variable elastic moduli and density. There are a number of works that are devoted to the study of direct problems for given laws of properties of an inhomogeneous material [5–7]. In a number of cases, solutions were obtained numerically using the finite element method [8–10], and for some special cases, analytical solutions were obtained (see, for example [11–13]). One-dimensional or two-dimensional power functions described by one or two parameters are usually used as variation laws. In particular, a number of works study the behavior of inhomogeneous rods with properties that vary along one or two coordinates [14–16]. This is because rods remain one of the most common structural elements and are more accessible for full-scale experiments.

Considering the complexity and cost of FGM production, an important problem is to identify the real variation laws using nondestructive methods [17]. Among these methods, the acoustic method is worth noting. Compared to some others, it quickly allows us to carry out experiments, can be used for bodies of various shapes, and is cheaper. Within the framework of this method, it is assumed that the variable characteristics effect the acoustic properties of the object. The problem of diagnosing the properties of an inhomogeneous material can be considered as an inverse coefficient problem related to identifying the parameters of the differential operator that describe the behavior of an object.

From a mathematical point of view, such problems are usually essentially ill-posed and nonlinear. Inverse coefficient problems arise in many fields of science and engineering, including mechanics, biomechanics, physics, medicine, and geophysics [18,19]. The main difficulty is constructing operator relations that connect the input data and the desired functions or parameters of differential operators [18]. In some cases, inverse problems are reduced to minimizing the residual functional on the corresponding compact set constructed from a priori information about the sought-for quantities. On the other hand, there are more complex problems in which the search for unknown characteristics is carried out in a wide class of functions. The choice of special methods with which to solve such problems is determined based on the specific problem and the available data. Some commonly used methods are Tikhonov regularization, least-squares methods, Bayesian inversion and iterative processes. These methods can be computationally intensive, and the choice of method and associated parameters can have a significant impact on the accuracy and stability of the solution. Taking into account the features of inverse problems, the choice of the initial approximation in iterative processes is an important problem. The iterative process may not converge if it differs significantly from the desired function or parameter.

The most important applied problems solution methods are those that make it possible to search for unknown quantities in a wide class of functions in the presence of the input data error. Previously, the authors showed that in some cases, inverse coefficient problems of elasticity and thermoelasticity can be reduced to the study of the Fredholm integral equation (FIE) of the first kind [20,21].

The paper [22] provides an overview of numerical methods with which to solve the FIE of the first kind. The first part of the paper describes the importance of FIE analysis in various studies, the second part presents the main theoretical statements and definitions, the third one describes the existing numerical methods for solving these equations (direct numerical integration method, wavelet analysis, GMRES method, multistage iterative method, CAS wavelet solution, multiple constraint smoothing method, Tikhonov regularization, etc.), and the fourth provides a brief assessment of these and other methods, including heuristic methods (genetic algorithm, neural networks, etc.). Other methods for solving integral equations of the first kind are also being developed (see, for example [23,24]). Each method has its own characteristics.

Among the most common methods used to construct a numerical solution of the FIE of the first kind, Tikhonov regularization should be noted. Theoretical foundations, program algorithms, and examples are presented in [25,26]. This method allows one to search for solutions of the FIE of the first kind, which arise as problems in various areas of study [27–29]. It should also be noted that Tikhonov regularization continues to develop (see, for example [30,31]).

In the present work, problems on longitudinal and flexural vibrations of an inhomogeneous rod are formulated. It is assumed that the Young's modulus and density are variable along the longitudinal coordinate. Direct problems of determining longitudinal and transverse displacements were solved numerically. The effect of variable properties on amplitude-frequency characteristics (AFC) was analyzed. Sensitivity analysis was carried out. A new inverse problem on the simultaneous identification of the variation laws of Young's modulus and density from AFC data, which are measured in given frequency ranges, is considered. A numerical solution using an iterative process is proposed. A system of FIE of the first kind is derived for its implementation. The solution was obtained

using the Tikhonov method and the LSQR method. To demonstrate the accuracy of the obtained solutions, reconstruction examples are presented.

**2. Formulation of the System of FIE of the First Kind**

Consider the problem of determining the variation laws of the elastic modulus  $E(x)$  and density  $\rho(x)$  of an inhomogeneous elastic rod. Within the framework of acoustic diagnostics, the identification of these variable properties can be carried out given the data on the AFC change. Since two functions are unknown, we will consider problems of steady-state longitudinal (Problem 1) and flexural (Problem 2) vibrations. The rod length equals  $l$ . The left end of the rod is rigidly fixed. Vibrations are forced by concentrated forces applied at the right end (see Figure 1).

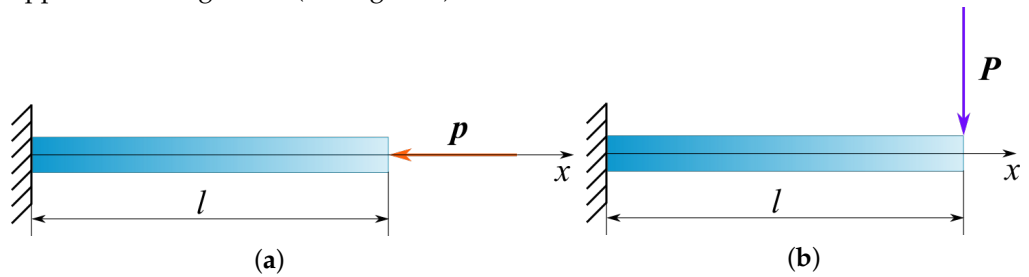


Figure 1. Inhomogeneous rod with applied longitudinal (a) and transverse (b) forces.

**Problem 1.** Longitudinal vibrations of the rod are described as follows:

$$\begin{cases} (EFw_1')' + \rho\omega^2 Fw_1 = 0 \\ w_1(0) = 0 \\ EFw_1'(l) = p \end{cases} \quad \text{or} \quad \begin{cases} s' = -\lambda\eta u \\ u' = \frac{s}{g} \\ u(0) = 0 \\ s(1) = p_* \end{cases}, \tag{1}$$

where  $\xi = x/l \in [0, 1]$ ,  $w_1(x) = lu(\xi)$ ,  $E(x) = E_*g(\xi)$ ,  $\rho(x) = \rho_*\eta(\xi)$ ,  $\lambda = \rho_*\omega^2 l^2 / E_*$ ,  $p_* = p / (E_*F)$ . Here,  $u$  is the displacement function along the rod axis,  $F$  is the cross-sectional area,  $\omega$  is the vibration frequency, and the coefficients  $E_*$  and  $\rho_*$  represent characteristic values of Young’s modulus and density, respectively. The functions  $g(\xi)$  and  $\eta(\xi)$  describe the laws of variation of variable characteristics; the parameter  $\lambda$  is proportional to the vibration frequency.

**Problem 2.** Flexural vibrations of the rod

$$\begin{cases} (JEw_2'')'' - \rho\omega^2 Fw_2 = 0 \\ w_2(0) = 0 \\ w_2'(0) = 0 \\ (JEw_2'')(l) = 0 \\ (JEw_2'')'(l) = -P \end{cases} \quad \text{or} \quad \begin{cases} a' = \gamma\lambda\eta v \\ b' = a \\ c' = \frac{b}{g} \\ v' = c \\ a(1) = p^* \\ b(1) = 0 \\ c(0) = 0 \\ v(0) = 0 \end{cases}, \tag{2}$$

where similar notations are introduced

$$w_2(x) = lv(\xi), \gamma = \frac{Fl^2}{J}, p^* = -\frac{Pl^2}{JE_*}.$$

Here,  $v$  is the function of the vertical displacement of points on the rod axis and  $J$  is the axial moment of inertia of the cross section. For rods of circular cross-section with radius  $r$ , the value of the  $\gamma$  parameter is defined as  $\gamma = 4l^2 / r^2$ . Within the framework of beam theory, it is usually assumed that  $r/l \leq 1/5$ , so the value of the parameter  $\gamma \geq 100$ . Hereinafter, we will assume that  $\gamma = 100$ .

Each of these problems for given functions  $g(\xi), \eta(\xi)$  can be solved numerically; for example, using the shooting method [32].

The solution of the inverse problem consists of determining the functions  $g(\xi), \eta(\xi)$  and  $u(\xi), v(\xi)$  from the data on the AFC change  $u(1, \lambda) = f(\lambda), v(1, \lambda) = q(\lambda)$ , specified at different frequency ranges  $\lambda \in [\lambda_1^-, \lambda_1^+]$  and  $\lambda \in [\lambda_2^-, \lambda_2^+]$ , respectively. This problem is essentially nonlinear. To solve it, the technique described in [33], based on the linearization method is used.

Functions describing displacement and parameter changes are represented as follows

$$\begin{aligned} g(\xi) &= g_0(\xi) + \varepsilon g_1(\xi), \eta(\xi) = \eta_0(\xi) + \varepsilon \eta_1(\xi), \\ u(\xi) &= u_0(\xi) + \varepsilon u_1(\xi), v(\xi) = v_0(\xi) + \varepsilon v_1(\xi), \end{aligned} \tag{3}$$

where  $g_1(\xi), \eta_1(\xi)$  are corrections to the corresponding functions,  $\varepsilon$  is the small formal parameter. To determine these, a system of two FIEs of the first kind can be obtained from the generalized reciprocity relation [20,33]:

$$\begin{cases} \int_0^1 (g_1(\xi)K_{11}(\xi, \lambda) - \eta_1(\xi)K_{12}(\xi, \lambda))d\xi = F_1(\lambda), & \lambda \in [\lambda_1^-, \lambda_1^+] \\ \int_0^1 (g_1(\xi)K_{21}(\xi, \lambda) - \eta_1(\xi)K_{22}(\xi, \lambda))d\xi = F_2(\lambda), & \lambda \in [\lambda_2^-, \lambda_2^+] \end{cases}, \tag{4}$$

where  $K_{11}(\xi, \lambda) = (u'_0)^2, K_{12}(\xi, \lambda) = \lambda u_0^2, K_{21}(\xi, \lambda) = (v'_0)^2, K_{22}(\xi, \lambda) = \gamma \lambda v_0^2$  — non-negative kernels of integral operators,  $F_1(\lambda) = -p_*(f(\lambda) - u_0(1, \lambda)), F_2(\lambda) = p_*(q(\lambda) - v_0(1, \lambda))$ , the functions  $u_0(\xi)$  and  $v_0(\xi)$  are determined numerically from the solution of the following boundary value problems for the given laws  $\eta_0$  and  $g_0$

$$\begin{cases} s'_0 = -\lambda \eta_0 u_0 \\ u'_0 = \frac{s_0}{g_0} \\ u_0(0) = 0 \\ s_0(1) = p_* \end{cases}, \begin{cases} a'_0 = \gamma \lambda \eta_0 v_0 \\ b'_0 = a_0 \\ c'_0 = \frac{b_0}{g_0} \\ v'_0 = c_0 \\ a_0(1) = p^* \\ b_0(1) = 0 \\ c_0(0) = 0 \\ v_0(0) = 0 \end{cases}. \tag{5}$$

It should be noted that kernels of these equations are non-negative. The right-hand sides of the equations are the differences in the AFC values calculated at the frequency ranges. Therefore, the effect of the Young’s modulus and density variation laws on the values of the AFC and kernels is an important aspect to consider when constructing a numerical scheme to solve this system.

### 3. Sensitivity Analysis

To analyze the effect of the density variation laws  $\eta(\xi)$  on the AFC of an inhomogeneous rod, graphs of the functions  $u(1, \lambda)$  and  $v(1, \lambda)$  in the vicinity of the first resonance for two pairs of material properties variation laws are presented (see Figure 2):  $g_1(\xi) = 1 + 0.5 e^{-\xi}, \eta_1(\xi) = 1$  (black solid lines) and  $g_2(\xi) = 1 + 0.5e^{-\xi}, \eta_2(\xi) = 1 + \xi$  (green dash-dotted lines). Here and below, without loss of generality, taking into account the linearity of the problem, we assume that  $p^* = p_* = 1$ .

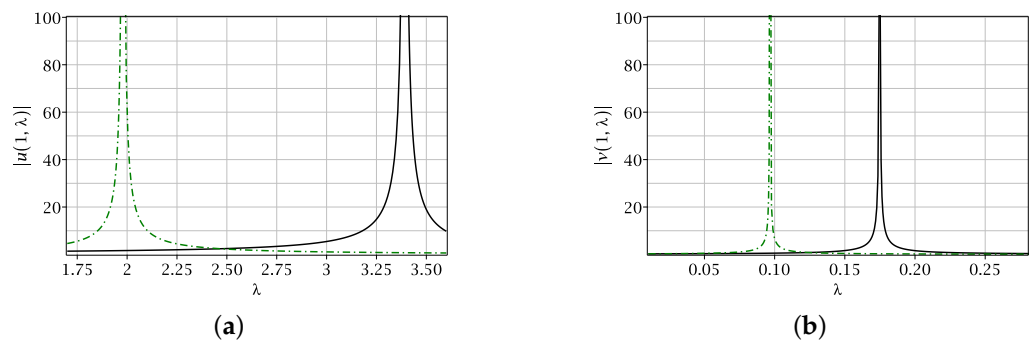


**Figure 2.** AFC  $|u(1, \lambda)|$  (a) and  $|v(1, \lambda)|$  (b) in the vicinity of the first resonance for two variation laws for the density.

To estimate the effect of the Young’s modulus variation laws  $g(\xi)$ , the graphs  $u(1, \lambda)$  and  $v(1, \lambda)$  in the vicinity of the first resonance for two pairs of material properties variation laws are similarly presented (see Figure 3):  $g_1(\xi) = 1, \eta_1(\xi) = 1 + \xi$  (black solid lines) and  $g_2(\xi) = 1 + 0.5e^{-\xi}, \eta_2(\xi) = 1 + \xi$  (green dash-dotted lines). Similar AFC change results were also obtained in the vicinity of the second resonances.

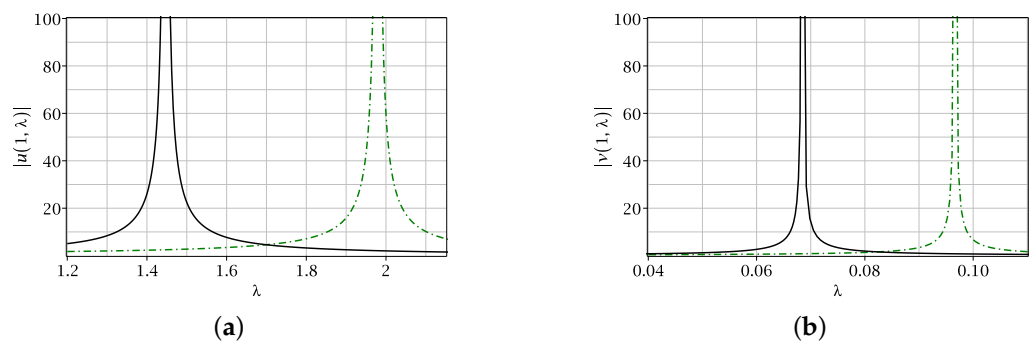


**Figure 3.** AFC  $|u(1, \lambda)|$  (a) and  $|v(1, \lambda)|$  (b) in the vicinity of the first resonance for two variation laws for the Young’s modulus.

As it can be seen from the presented results, the Young’s modulus and density variation laws have a commensurate effect on the AFC values for the considered problems. In this case, the largest change occurs in the vicinity of the resonant frequencies. To reveal the peculiarities of the kernels  $K_{ij}(\xi, \lambda)$  of the integral operators (4) on the basis of numerical solutions to direct problems, their graphs are built on the frequency ranges that are below the first (see Figure 4) and between the first and second resonances (see Figure 5). It can be seen from these figures that below the first resonance, all the graphs are monotonic, and between resonances they are non-monotonic. The kernels  $K_{12}(\xi, \lambda)$  and  $K_{22}(\xi, \lambda)$  vanish for  $\xi = 0$  and for the kernel  $K_{21}(\xi, \lambda) = 0$  for  $\xi = 1$  due to the boundary conditions. These features must be taken into account when constructing a numerical solution to the considered inverse coefficient problem. It should be noted that some peculiarities can be avoided by changing the boundary conditions. For example, when flexural vibrations are caused by a bending moment applied at the right end, the kernel is  $K_{21}(1, \lambda) \neq 0$ . As can be seen from the presented graphs, a sharp change in the values of the kernels is observed near the resonance frequencies. These zones are the most informative in the study of inverse coefficient problems, since the effect of variable properties on acoustic characteristics is significantly noticeable.

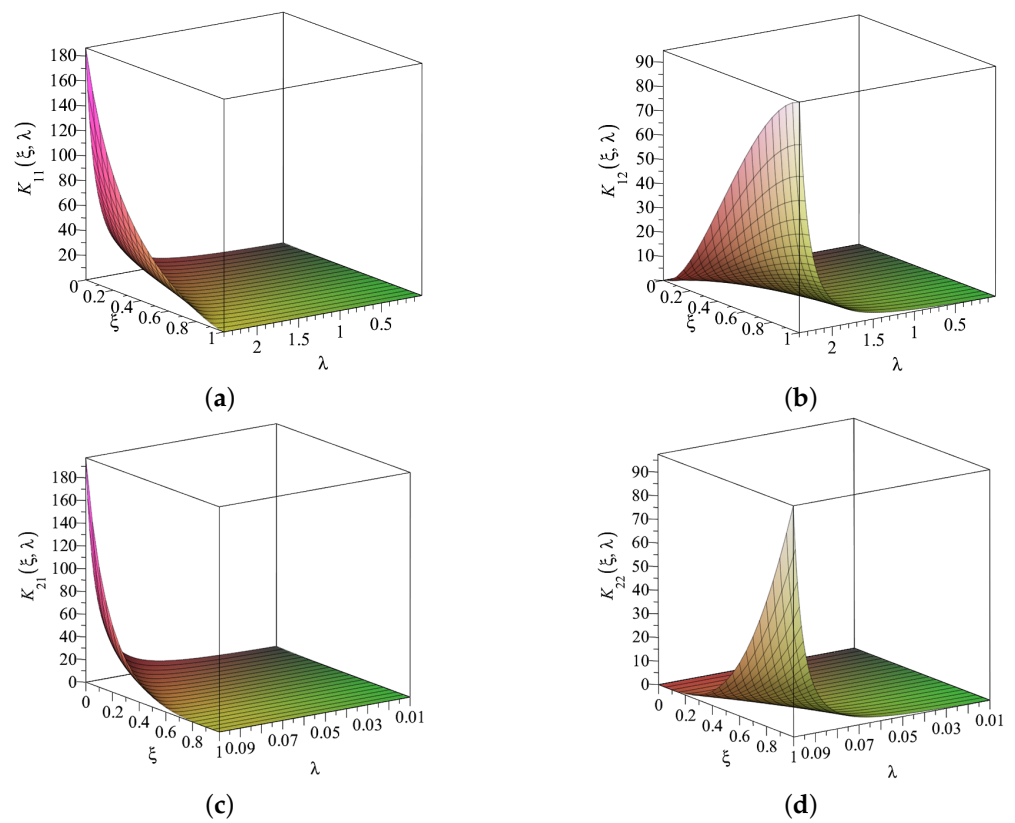


**Figure 4.** Kernels  $K_{ij}(\xi, \lambda)$  below the first resonance: (a)  $K_{11}(\xi, \lambda)$ , (b)  $K_{12}(\xi, \lambda)$ , (c)  $K_{21}(\xi, \lambda)$ , (d)  $K_{22}(\xi, \lambda)$ .

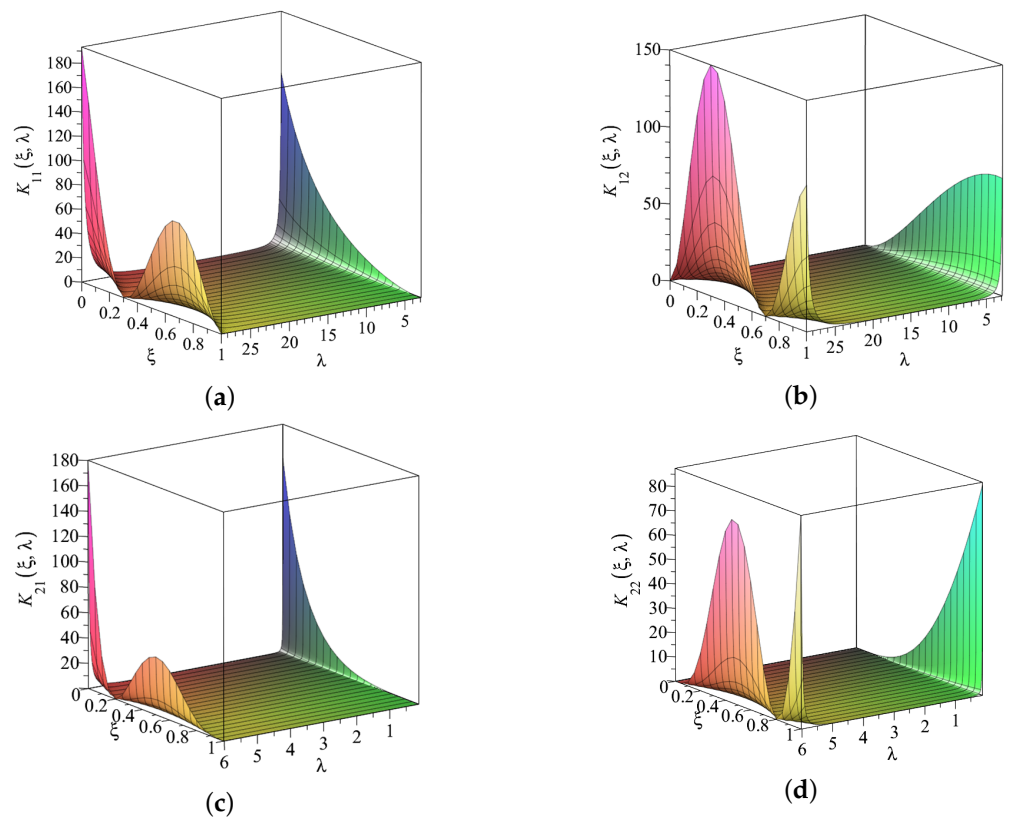


**Figure 5.** Kernels  $K_{ij}(\xi, \lambda)$  between the first and the second resonances: (a)  $K_{11}(\xi, \lambda)$ , (b)  $K_{12}(\xi, \lambda)$ , (c)  $K_{21}(\xi, \lambda)$ , (d)  $K_{22}(\xi, \lambda)$ .

#### 4. Iterative Process Implementation

Now, using the equation system (4), we can construct an iterative process for mechanical parameters reconstruction. Taking into account the ill-posed nature of the inverse problem and the variation laws effect on the right-hand sides of the equations, it should be noted that an important stage is the initial approximation choice. Basing on a priori information about the reconstructed functions boundedness, we consider the following three approaches:

1. Genetic algorithm. We approximate unknown functions using the Lagrange polynomial

$$\begin{aligned}
 g(\xi) &= 1 + \sum_{i=1}^N g_i \prod_{j=0, j \neq i}^N \frac{\xi - \xi_j}{\xi_j - \xi_i} \\
 \eta(\xi) &= 1 + \sum_{i=1}^N \eta_i \prod_{j=0, j \neq i}^N \frac{\xi - \xi_j}{\xi_j - \xi_i}
 \end{aligned}
 \tag{6}$$

where  $\xi_i = ih$  — equidistant nodes,  $g_i, \eta_i$  — real coefficients of the corresponding representations,  $i = 0, 1 \dots N, h = 1/N$ .

Consider the following objective function:

$$\begin{aligned}
 J(\eta_0, \dots, \eta_n, g_0, \dots, g_n) &= \sum_{i=0}^n \left[ U(\eta_0, \dots, \eta_n, g_0, \dots, g_n, \lambda_1^{(i)}) - f(\lambda_1^{(i)}) \right]^2 \\
 &+ \sum_{j=0}^m \left[ V(\eta_0, \dots, \eta_n, g_0, \dots, g_n, \lambda_2^{(j)}) - q(\lambda_2^{(j)}) \right]^2,
 \end{aligned}
 \tag{7}$$

where  $\lambda_1^{(i)} \in [\lambda_1^-, \lambda_1^+], i = 1, 2 \dots n, \lambda_2^{(j)} \in [\lambda_2^-, \lambda_2^+], j = 1, 2 \dots m$ , the values of  $U$  and  $V$  are equal to the values of  $u(1, \lambda_1^{(i)})$  and  $v(1, \lambda_2^{(j)})$ , respectively. These values were obtained numerically from the solution of the problems (1) and (2) for each set of parameters  $(\eta_0, \dots, \eta_n, g_0, \dots, g_n)$ .

Thus, the initial approximations search in the form (6) is reduced to the objective function minimization. Each set of numbers  $(\eta_0, \dots, \eta_n, g_0, \dots, g_n)$  is represented as a sequence of bits, consisting of zeros and ones. The search for a solution is carried out using the genetic algorithm GALGO-2.0, implemented in C++ [34]. The choice of the C++ is due to the high speed with which numerical solutions to problems (1) and (2) are obtained using the shooting method.

2. Minimization of the residual functional on a compact set. It should be noted that, in a particular case, the problem of finding initial approximations in the class of linear functions of the form

$$g(\xi) = a_g + b_g \xi, \quad \eta(\xi) = a_\eta + b_\eta \xi
 \tag{8}$$

can be reduced to finding the minimum of a function for a set of parameters  $(a_g, b_g, a_\eta, b_\eta)$  on compact sets  $M_g$  and  $M_\eta$ . These sets are constructed using a priori information about the boundedness of the sought-for functions  $0 < g^- \leq g(\xi) \leq g^+, 0 < \eta^- \leq \eta(\xi) \leq \eta^+, \xi \in [0, 1]$  (see Figure 6). The numerical implementation of this approach is carried out by calculating the values of the function  $J$  for each set  $(a_g, b_g, a_\eta, b_\eta)$  on the grids of the compact sets  $M_g$  and  $M_\eta$  and choosing the set that minimizes the function  $J$ . The step of compact sets partitioning has a significant effect on the accuracy of the parameters  $a_g, b_g, a_\eta, b_\eta$  obtained.

3. Additional information about the values of the sought-for functions. The initial approximation of the restored function can be chosen in the form of a constant, which is defined as the arithmetic mean of the maximum and minimum values, or as equal to one of them. The main advantage of this approach is its ease of implementation. On the other hand, the initial approximation chosen this way can differ significantly from the exact solution, which can lead to a divergence of the iterative process.

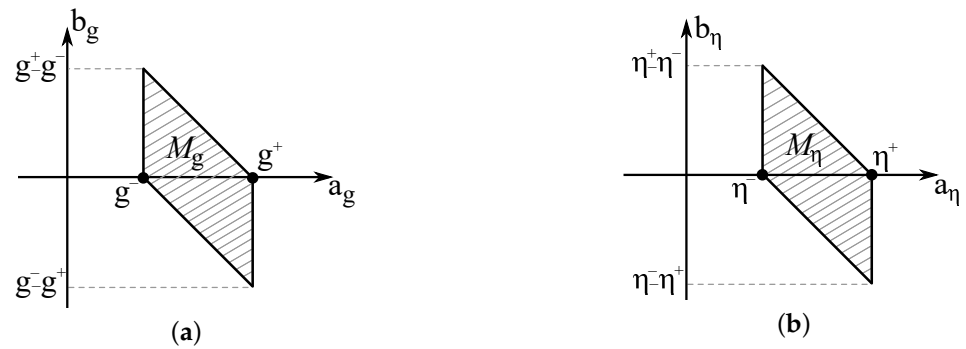


Figure 6. Compact sets  $M_g$  (a) and  $M_\eta$  (b).

Now, we formulate the iterative process to find the functions of Young’s modulus and density. At the first stage, an initial approximation is selected according to one of the methods described above. Next, corrections to the sought-for functions are determined from the solution of the system of FIEs. The corrections to the corresponding functions are made. Then, the process is closed and repeated until the stopping condition is reached: this is the maximum predetermined number of iterations or the smallness of the right-hand sides of FIEs. It should be noted that the main difficulty in the implementation of this process lies in the construction of a numerical solution to the system of FIEs. Since such a problem is essentially ill-posed, it is necessary to use special techniques. In this paper, the Tikhonov regularization and the LSQR method are considered. The system of linear algebraic equations of size  $2n$  for the implementation of Tikhonov regularization is presented:

$$B^\alpha u = F, \tag{9}$$

where

$$B^\alpha = B + \alpha C, \quad C = E + \begin{pmatrix} C_1 & 0 \\ 0 & C_1 \end{pmatrix},$$

$$F = \begin{pmatrix} f_1 \\ \vdots \\ f_{2n} \end{pmatrix}, \quad u = \begin{pmatrix} u_1 \\ \vdots \\ u_{2n} \end{pmatrix}, \quad B = \begin{pmatrix} b_{11} & \dots & b_{1n} \\ \vdots & \ddots & \vdots \\ b_{2n1} & \dots & b_{2n2n} \end{pmatrix}, \quad B = h_\xi h_\lambda A^T A$$

$$\xi_j = (j - 1)h_\xi, h_\xi = (n - 1)^{-1}, j = 1 \dots n,$$

$$f_k = h_\lambda \sum_{i=1}^{2m} \tilde{f}_i a_{ik}, \quad k = 1 \dots 2n,$$

$$\tilde{f}_i = \begin{cases} F_1(\lambda_i), & i = 1 \dots m, \\ F_2(\lambda_{i-m}), & i = m + 1 \dots 2m, \end{cases}$$

$$u_j = \begin{cases} g_1(\xi_j), & j = 1 \dots n, \\ \eta_1(\xi_{j-n}), & j = n + 1 \dots 2n, \end{cases}$$

$$a_{ij} = \begin{cases} K_{11}(\xi_j, \lambda_i), & i = 1 \dots m, j = 1 \dots n, \\ K_{12}(\xi_{j-n}, \lambda_i), & i = 1 \dots m, j = n + 1 \dots 2n, \\ K_{21}(\xi_j, \lambda_{i-m}), & i = m + 1 \dots 2m, j = 1 \dots n, \\ K_{22}(\xi_{j-n}, \lambda_{i-m}), & i = m + 1 \dots 2m, j = n + 1 \dots 2n, \end{cases}$$

$$C_1 = \begin{pmatrix} \frac{1}{h_\xi^2} & -\frac{1}{h_\xi^2} & 0 & \dots & 0 & 0 \\ -\frac{1}{h_\xi^2} & \frac{2}{h_\xi^2} & -\frac{1}{h_\xi^2} & \dots & 0 & 0 \\ \dots & \dots & \dots & \dots & \dots & \dots \\ 0 & 0 & \dots & -\frac{1}{h_\xi^2} & \frac{2}{h_\xi^2} & -\frac{1}{h_\xi^2} \\ 0 & 0 & \dots & 0 & -\frac{1}{h_\xi^2} & \frac{1}{h_\xi^2} \end{pmatrix}.$$

Here,  $E$  is the identity matrix,  $\alpha$  is the regularization parameter, and  $C_1$  is the  $n \times n$  band matrix. The  $\alpha$  parameter is determined according to the algorithm described [25].

The LSQR method is applied to a system of linear algebraic equations obtained after the discretization of the integral operators included in both equations. In this case, the trapezoidal rule was used. The LSQR method was implemented in the C++ according to the algorithm described in [35].

### 5. Reconstruction Examples

As a model example of the proposed methods for solving FIE systems, the reconstruction examples for monotonic and non-monotonic functions  $g(\xi)$  and  $\eta(\xi)$  are presented.

In Figures 7–15, there are results of reconstruction, maximum relative error and the corresponding AFC.

In Figures 7, 10 and 13, we plot the exact solutions (black solid lines), initial approximations (red open circles) and the reconstructed solutions obtained using the LSQR method [35] (green circles) and an iterative process based on the Tikhonov regularization (blue dash-dotted lines).

Hereinafter, the maximum relative error of  $g(\xi)$  reconstruction is determined by  $\delta(\xi_i) = \frac{|g_*(\xi_i) - g_e(\xi_i)|}{\max_{\xi \in [\xi_0, 1]} g_e(\xi)} \cdot 100\%$ ,  $\xi_i \in [\xi_0, 1]$ , and similarly for  $\eta(\xi)$ . Graphs of  $\delta(\xi)$  for increasing, decreasing and non-monotonic laws  $g(\xi)$  and  $\eta(\xi)$  are shown in Figures 8, 11 and 14, respectively.

In Figures 9, 12 and 15 the AFC  $|u(1, \lambda)|$  and  $|v(1, \lambda)|$  are plotted in the frequency ranges in which the identification of the sought-for variation laws is carried out. It is worth noting that in all examples, there is a significant convergence of the AFC for the exact and regularized solutions.

Figure 7 (monotonically increasing laws): the exact laws are  $g_e(\xi) = 2 - (\xi - 1)^2$  and  $\eta_e(\xi) = 1 + e^{5(\xi-1)}$ , the initial approximations are  $g_f(\xi) = 1$  and  $\eta_f(\xi) = 1$  (minimums of reconstructed laws), reconstructed laws are  $g_*(\xi)$  and  $\eta_*(\xi)$ ; 20 iterations (Tikhonov regularization) and 100 iterations (LSQR method). The value of  $\delta$  is 5.3% for the function  $g(\xi)$  (at the right end is 7.5%) and 2.1% for function  $\eta(\xi)$  (at the right end is 8.1%). The frequency ranges are  $\lambda \in [0, 1.44]$  for  $g(\xi)$ , and  $\lambda \in [0, 0.02]$  for  $\eta(\xi)$ . The number of points along the longitudinal coordinate is  $n = 31$ ; the number of points in frequency is  $m = 11$ . The residual norm of the right-hand sides to exit the iterative process is equal to  $10^{-7}$ .

Figure 10 (monotonically decreasing laws): the exact laws are  $g_e(\xi) = 2 - (\xi - \xi_0)^2$  and  $\eta_e(\xi) = 1 + e^{-4\xi+0.02}$ , the initial approximations are  $g_0(\xi) = \eta_0(\xi) = 2 - \xi$ ; 10 iterations (Tikhonov regularization) and 26 iterations (LSQR method). The value of the relative error  $\delta$  is 3.58% for the function  $g(\xi)$  and 6.44% for the function  $\eta(\xi)$ . The frequency ranges are  $\lambda \in [6.25, 16.0]$  for  $g(\xi)$ , and  $\lambda \in [0.71, 3.75]$  for  $\eta(\xi)$ . The number of division points and the residual norm are similar to those in the previous example.

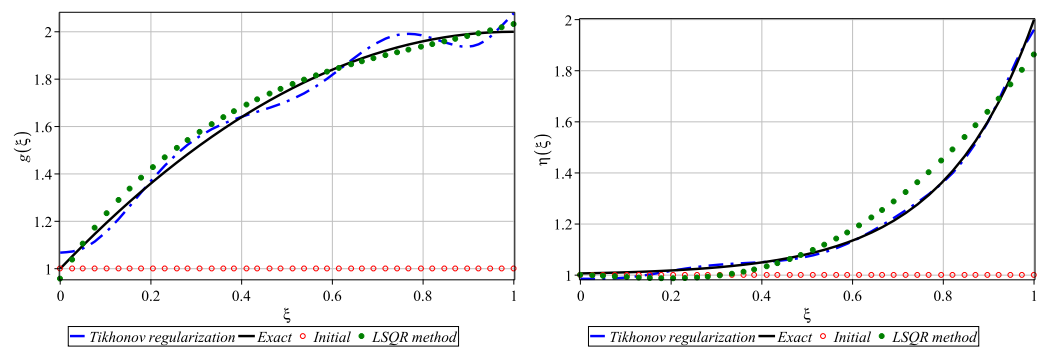


Figure 7. Reconstruction of monotonically increasing laws.

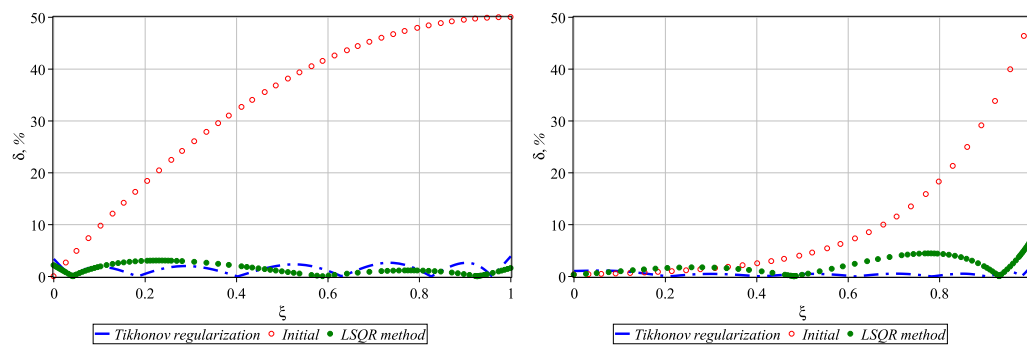


Figure 8. The value of the relative error  $\delta$ : function  $g(\xi)$  (left), function  $\eta(\xi)$  (right).

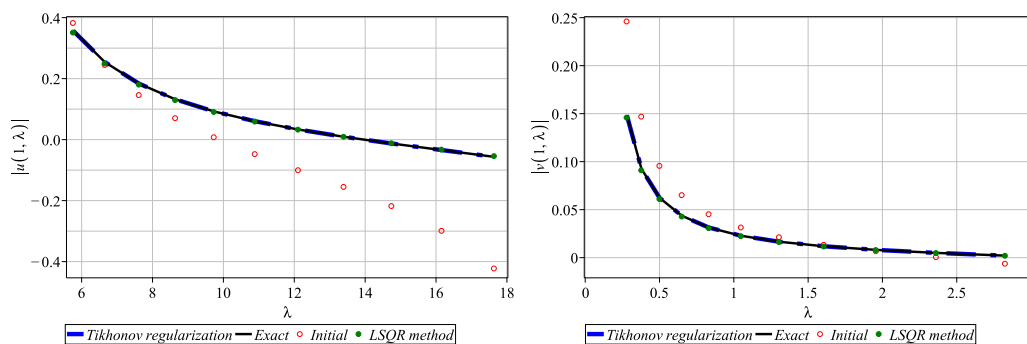


Figure 9. AFC  $|u(1, \lambda)|$  (left) and  $|v(1, \lambda)|$  (right).

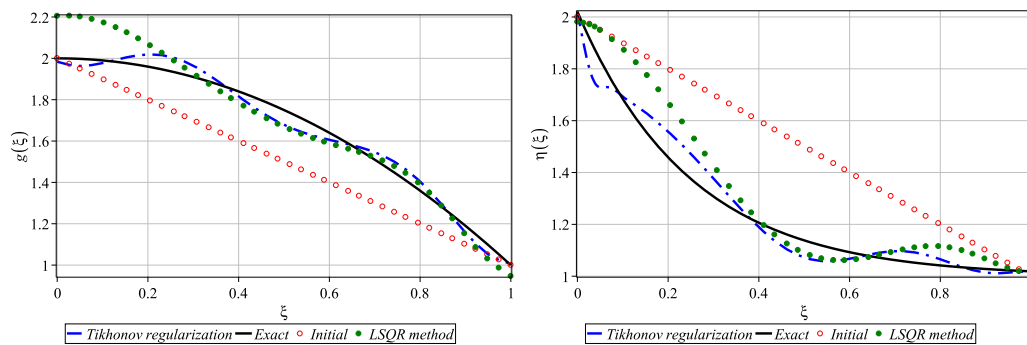


Figure 10. Reconstruction of monotonically decreasing functions.

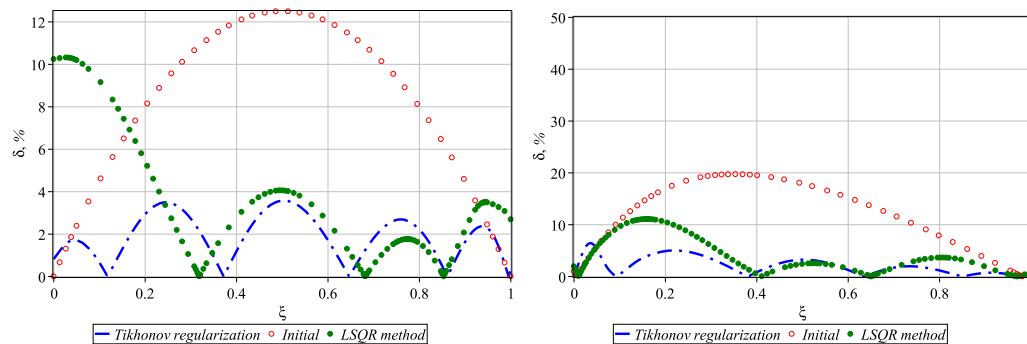


Figure 11. The value of the relative error  $\delta$ : function  $g(\xi)$  (left), function  $\eta(\xi)$  (right).

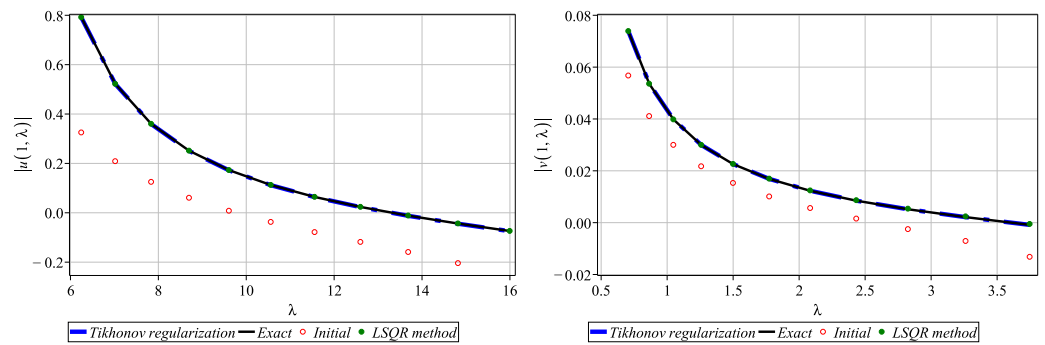


Figure 12. AFC  $|u(1, \lambda)|$  (left) and  $|v(1, \lambda)|$  (right).

Reconstruction of non-monotonic laws is presented in the Figure 13. The exact laws are  $g_e(\xi) = 1 + \sin(\pi\xi)$  and  $\eta_e(\xi) = 4\xi^2 - 4\xi + 2$ , the initial approximations are  $g_0(\xi) = \eta_0(\xi) = 1.5$  (average values); 15 iterations (Tikhonov regularization) and 23 iterations (LSQR method). The value of  $\delta$  is 3.9% for the function  $g(\xi)$  and 4.09% for the function  $\eta(\xi)$  (at the left end is 27%). The frequency ranges are  $\lambda \in [4.41, 15.21]$  for  $g(\xi)$  and  $\lambda \in [0.19, 2.31]$  for  $\eta(\xi)$ .

It can be seen from the presented results that the proposed numerical methods for solving the system of FIEs of the first kind allow one to obtain similar results. It should be noted that the initial approximation choice has a significant effect on the reconstruction accuracy. The largest error in the reconstruction of the non-monotonic function  $\eta(\xi)$  is due to the peculiarity of the corresponding kernels  $K_{12}, K_{22}$ . Due to the boundary conditions, they vanish at  $\xi = 0$ .

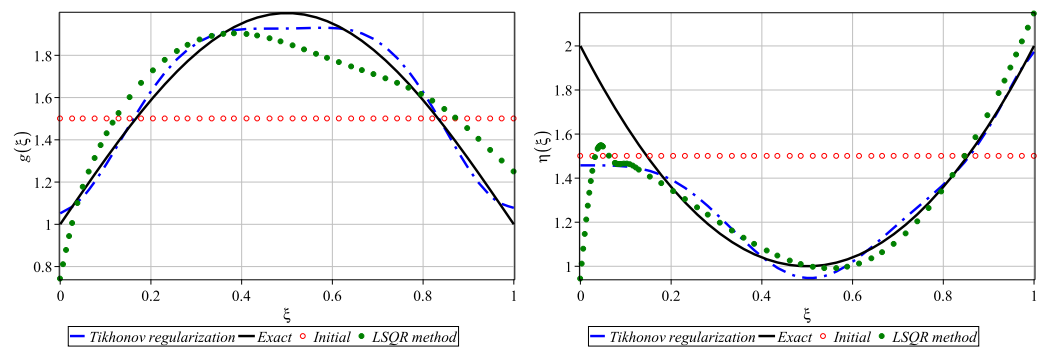


Figure 13. Reconstruction of non-monotonic functions.

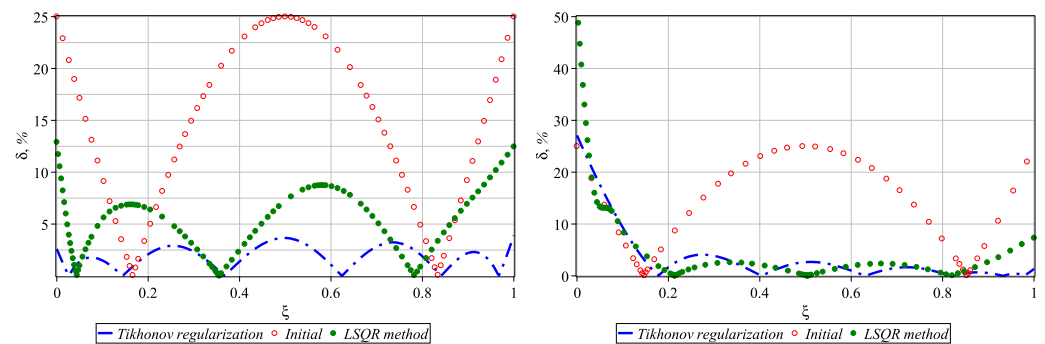


Figure 14. The value of the relative error  $\delta$ : function  $g(\xi)$  (left), function  $\eta(\xi)$  (right).

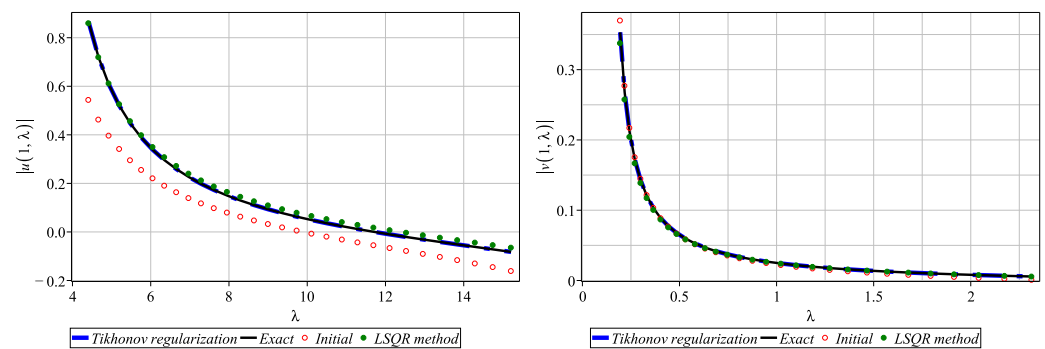


Figure 15. AFC  $|u(1, \lambda)|$  (left) and  $|v(1, \lambda)|$  (right).

## 6. Discussion

In this article, direct problems of steady-state longitudinal and flexural vibrations of an inhomogeneous rod are considered. Its properties are described using the Young's modulus and density varying along the longitudinal coordinate. The solution to the direct problem in the general case of properties inhomogeneity is reduced to a numerical study of the corresponding canonical systems of differential equations with variable coefficients using the shooting method. This method allows us to obtain a solution with a given accuracy. The proposed method allows us to consider a wider class of inhomogeneity laws (continuous monotonic and non-monotonic, discontinuous, etc.) in comparison with other numerical solutions to these problems. Unlike the original statement of the problem, there is no need to calculate derivatives of these functions. Based on the proposed numerical solution to the direct problem, a sensitivity analysis was carried out by estimating the effect of the variable Young's modulus and density on the AFC measured at the right end of the rod. The analysis revealed that this influence is more significant in the vicinity of resonances. A new inverse coefficient problem on the simultaneous identification of variation laws of Young's modulus and density from AFC data for problems of longitudinal and flexural vibrations of a rod is considered. The AFC is measured at specified frequency ranges. The solution was obtained using the iterative method. The initial approximations were selected in the class of linear functions. It should be noted that in several practical problems, such an approximation can be chosen as the final solution. To find the initial approximation, several approaches are proposed: a genetic algorithm, minimization of the residual functional on a compact set, additional information about the values of the sought-for functions at the ends of the rod. A new system of FIE of the first kind with smooth non-negative kernels to find two unknown corrections is obtained using a previously tested technique. The kernels are plotted, and their features are revealed. Since solving the FIE of the first kind is an ill-posed problem, the Tikhonov method and LSQR are used. The systems of algebraic equations obtained after discretization of integral operators are presented. Reconstruction examples demonstrate the effectiveness of the proposed approach are presented. It is shown that in some cases, the Tikhonov method and LSQR give similar reconstruction results. Features of solutions associated with boundary conditions are noted (the kernels of integral operators vanish). Practical recommendations to choose the optimal frequency range and implement the reconstruction procedure effectively are proposed.

## 7. Conclusions

Methods for analyzing inverse coefficient problems of mechanics by reconstructing two variation laws in material characteristics within the framework of the acoustic sounding method are presented. It is shown that they can be reduced to the implementation of iterative processes, and at each iteration, a direct problem with known changes in characteristics is solved and corrections are found from solutions to an ill-posed problem that involves constructing a solution for a system of two FIEs of the first kind with smooth non-negative kernels. As specific examples, the paper considers the problems of longitudinal and flexural vibrations of an inhomogeneous rod, where the unknown characteristics are the Young's

modulus and density. An analysis of changes in the kernels of integral equations obtained as a result of linearization for different values of the frequency parameter is carried out, and the features of their structure are revealed. Two numerical methods for solving the FIE system of the first kind are presented. The first method is based on the Tikhonov regularization; the second one is based on the LSQR method. To test the proposed numerical schemes, the results of the reconstruction of monotonic and non-monotonic functions are presented. A comparative assessment of the accuracy of the results obtained is provided.

**Author Contributions:** A.V.: formulation of integral relations; P.U.: software, visualization; V.D.: methodology, investigation, validation, writing—review and editing; R.M.: software, visualization, writing—review and editing. All authors have read and agreed to the published version of the manuscript.

**Funding:** The study was supported by the grant of the Russian Science Foundation № 22-11-00265, <https://rscf.ru/en/project/22-11-00265/> (accessed on 1 September 2023) in the Southern Federal University.

**Data Availability Statement:** On reasonable request, the corresponding authors will provide the data sets utilized in this paper.

**Conflicts of Interest:** The authors declare no conflict of interest.

## References

- Boggarapu, V.; Gujjala, R.; Ojha, S.; Acharya, S.; Venkateswara babu, P.; Chowdary, S.; kumar Gara, D. State of the art in functionally graded materials. *Compos. Struct.* **2021**, *262*, 113596. [[CrossRef](#)]
- Saleh, B.; Jiang, J.; Fathi, R.; Al-hababi, T.; Xu, Q.; Wang, L.; Song, D.; Ma, A. 30 Years of functionally graded materials: An overview of manufacturing methods, Applications and Future Challenges. *Compos. Part B Eng.* **2020**, *201*, 108376. [[CrossRef](#)]
- Naebe, M.; Shirvanimoghaddam, K. Functionally graded materials: A review of fabrication and properties. *Appl. Mater. Today* **2016**, *5*, 223–245. [[CrossRef](#)]
- Birman, V.; Byrd, L.W. Modeling and Analysis of Functionally Graded Materials and Structures. *Appl. Mech. Rev.* **2007**, *60*, 195–216. [[CrossRef](#)]
- Birsan, M.; Altenbach, H.; Sadowski, T.; Eremeyev, V.; Pietras, D. Deformation analysis of functionally graded beams by the direct approach. *Compos. Part B Eng.* **2012**, *43*, 1315–1328. [[CrossRef](#)]
- Demir, E.; Sayer, M.; Callioglu, H. An approach for predicting longitudinal free vibration of axially functionally graded bar by artificial neural network. *Proc. Inst. Mech. Eng. Part C J. Mech. Eng. Sci.* **2022**, *237*, 2245–2255. [[CrossRef](#)]
- Xue, C.X.; Pan, E. On the longitudinal wave along a functionally graded magneto-electro-elastic rod. *Int. J. Eng. Sci.* **2013**, *62*, 48–55. [[CrossRef](#)]
- Marzavan, S.; Nastasescu, V. Free Vibration Analysis of a Functionally Graded Plate by Finite Element Method. *Ain Shams Eng. J.* **2023**, *14*, 102024. [[CrossRef](#)]
- Vatulyan, A.O.; Dudarev, V.V.; Mnukhin, R.M. Functionally graded cylinders: Vibration analysis. *ZAMM-J. Appl. Math. Mech./Z. Für Angew. Math. Und Mech.* **2023**, e202200430.
- Alshorbagy, A.E.; Eltahir, M.; Mahmoud, F. Free vibration characteristics of a functionally graded beam by finite element method. *Appl. Math. Model.* **2011**, *35*, 412–425. [[CrossRef](#)]
- Das, P.; Islam, M.; Somadder, S.; Hasib, M. Analytical and numerical solutions of pressurized thick-walled FGM spheres. *Arch. Appl. Mech.* **2023**, *93*, 2781–2792. [[CrossRef](#)]
- Benslimane, A.; Bouzidi, S.; Methia, M. Displacements and stresses in pressurized thick-walled FGM cylinders: Exact and numerical solutions. *Int. J. Press. Vessel. Pip.* **2018**, *168*, 219–224. [[CrossRef](#)]
- Tang, A.Y.; Wu, J.X.; Li, X.F.; Lee, K. Exact frequency equations of free vibration of exponentially non-uniform functionally graded Timoshenko beams. *Int. J. Mech. Sci.* **2014**, *89*, 1–11. [[CrossRef](#)]
- Le, C.I.; Le, N.A.T.; Nguyen, D.K. Free vibration and buckling of bidirectional functionally graded sandwich beams using an enriched third-order shear deformation beam element. *Compos. Struct.* **2021**, *261*, 113309. [[CrossRef](#)]
- Banerjee, J.; Ananthapuvirajah, A. Free vibration of functionally graded beams and frameworks using the dynamic stiffness method. *J. Sound Vib.* **2018**, *422*, 34–47. [[CrossRef](#)]
- Şimşek, M. Bi-directional functionally graded materials (BDFGMs) for free and forced vibration of Timoshenko beams with various boundary conditions. *Compos. Struct.* **2015**, *133*, 968–978. [[CrossRef](#)]
- Ida, N.; Meyendorf, N. *Handbook of Advanced Nondestructive Evaluation*; Springer: Cham, Switzerland, 2019; p. 1626. [[CrossRef](#)]
- Isakov, V. *Inverse Problems for Partial Differential Equations*, 3rd ed.; Part of the Applied Mathematical Sciences Book Series; Springer: Cham, Switzerland, 2017.
- Hussain, A.; Faye, I.; Muthuvalu, M.S.; Tang, T.B.; Zafar, M. Advancements in Numerical Methods for Forward and Inverse Problems in Functional near Infra-Red Spectroscopy: A Review. *Axioms* **2023**, *12*, 326. [[CrossRef](#)]

20. Dudarev, V.; Vatulyan, A.; Mnukhin, R.; Nedin, R. Concerning an approach to identifying the Lamé parameters of an elastic functionally graded cylinder. *Math. Methods Appl. Sci.* **2020**, *43*, 6861–6870. [[CrossRef](#)]
21. Vatulyan, A.; Nesterov, S. Study of the Inverse Problems of Thermoelasticity for Inhomogeneous Materials. *Sib. Math. J.* **2023**, *64*, 699–706. [[CrossRef](#)]
22. Yuan, D.; Zhang, X. An overview of numerical methods for the first kind Fredholm integral equation. *SN Appl. Sci.* **2019**, *1*, 1178. [[CrossRef](#)]
23. Kulikov, E.K.; Makarov, A.A. A Method for Solving the Fredholm Integral Equation of the First Kind. *J. Math. Sci.* **2023**, *272*, 558–565. [[CrossRef](#)]
24. Elahi, M.R.; Mahmoudi, Y.; Shamloo, A.S.; Rad, M.J. On projection method for numerical solution of hypersingular integral equations of the first kind combined with quadrature methods. *Phys. Scr.* **2023**, *98*, 045229. [[CrossRef](#)]
25. Tikhonov, A.N.; Arsenin, V.Y. *Solution of Ill-Posed Problems*; Winston and Sons: Washington, DC, USA, 1977.
26. Tikhonov, A.N.; Goncharski, A.V.; Stepanov, V.V.; Yagola, A.G. *Numerical Methods for the Solution of Ill-Posed Problems*; Kluwer Academic Publishers: Dordrecht, The Netherlands, 1995.
27. Bouhamidi, A.; Enkhbat, R.; Jbilou, K. Conditional gradient Tikhonov method for a convex optimization problem in image restoration. *J. Comput. Appl. Math.* **2014**, *255*, 580–592. [[CrossRef](#)]
28. Yang, G.; Lizhi, X.; Baosong, W. TSVD and Tikhonov methods and influence factor analysis for NMR data in shale rock. *J. Pet. Sci. Eng.* **2020**, *194*, 107508. [[CrossRef](#)]
29. Abdulla, U.; Poteau, R. Identification of parameters in systems biology. *Math. Biosci.* **2018**, *305*, 133–145. [[CrossRef](#)]
30. Somaieh, M.; Eslahchi, M. Extension of Tikhonov regularization method using linear fractional programming. *J. Comput. Appl. Math.* **2020**, *371*, 112677. [[CrossRef](#)]
31. Chitra, M.; Santhosh, G.; Jidesh, P. Fractional Tikhonov regularization method in Hilbert scales. *Appl. Math. Comput.* **2021**, *392*, 125701. [[CrossRef](#)]
32. Polyanin, A.D.; Zaitsev, V.F. *Handbook of Ordinary Differential Equations: Exact Solutions, Methods, and Problems*; Chapman and Hall/CRC: New York, NY, USA, 2017.
33. Vatulyan, A.O. The theory of inverse problems in the linear mechanics of a deformable solid. *J. Appl. Math. Mech.* **2010**, *74*, 648–653. [[CrossRef](#)]
34. Mallet, O. GALGO-2.0. 2017. Available online: <https://github.com/olmallet81/GALGO-2.0> (accessed on 1 September 2023).
35. Paige, C.; Saunders, M. LSQR: An Algorithm for Sparse Linear Equation and Sparse Least Squares. *ACM Trans. Math. Softw.* **1982**, *8*, 43–71. [[CrossRef](#)]

**Disclaimer/Publisher's Note:** The statements, opinions and data contained in all publications are solely those of the individual author(s) and contributor(s) and not of MDPI and/or the editor(s). MDPI and/or the editor(s) disclaim responsibility for any injury to people or property resulting from any ideas, methods, instructions or products referred to in the content.